



INSTITUT DE FRANCE
Académie des sciences

Comptes Rendus

Mécanique


Duc-Tuan Ta, Thien-Phu Le and Michael Burman

Operational modal identification based on parallel factor decomposition with the presence of harmonic excitation

Volume 349, issue 3 (2021), p. 435-452

<https://doi.org/10.5802/crmeca.90>

© Académie des sciences, Paris and the authors, 2021.
Some rights reserved.

 This article is licensed under the
CREATIVE COMMONS ATTRIBUTION 4.0 INTERNATIONAL LICENSE.
<http://creativecommons.org/licenses/by/4.0/>



*Les Comptes Rendus. Mécanique sont membres du
Centre Mersenne pour l'édition scientifique ouverte*
www.centre-mersenne.org



Short paper / Note

Operational modal identification based on parallel factor decomposition with the presence of harmonic excitation

Duc-Tuan Ta^{✉*, a}, Thien-Phu Le^{✉ a} and Michael Burman^a

^a Université Paris-Saclay, Univ Evry, LMEE, 91020, Evry, France

E-mails: ductuan.ta@uni-evry.fr (D.-T. Ta), thienphu.le@univ-evry.fr (T.-P. Le), michael.burman@univ-evry.fr (M. Burman)

Abstract. One of the main difficulties of the operational modal analysis is to deal with underdetermined problems in which the number of sensors is less than the number of active modes. In the last decade, methods based on the PARAllel FACtor (PARAFAC) decomposition have attracted a lot of attention in the field of modal analysis because it has been proven that these methods can deal with underdetermined cases, as well as the presence of harmonic excitations. Moreover, in combination with kurtosis value as a harmonic indicator, this makes them more efficient in distinguishing between harmonic and structural components. However, it can lead to distorted results as it does not take into account the variation in the length of the covariance functions of the modal coordinates. Since the kurtosis values are estimated from these covariance functions, the length of the latter directly affects the kurtosis. To overcome this limit, the present study proposes to introduce the choice of the length of these functions based on their frequency and damping coefficient. This change improves the existing method by more efficient separating between harmonics and modal components. The proposed procedure is validated using numerical simulations, followed by ambient vibration measurements.

Keywords. Modal analysis, PARAFAC decomposition, Covariance function, Harmonic, Kurtosis.

Manuscript received 24th March 2021, revised 16th July 2021, accepted 19th July 2021.

1. Introduction

In recent decades, operational modal analysis (OMA) has been significantly developed, and it plays a vital role in the engineering fields. This is an identification technique that uses only structural responses without knowing the input excitation information [1]. It is a challenging task to measure the input excitations of mechanical systems and sometimes even impossible. Therefore, the input excitation is frequently considered as Gaussian white noise. However, this assumption is not always validated in reality because of the existence of periodic excitations. Moreover, the presence of input excitations such as harmonic ones can cause errors in the modal

* Corresponding author.

identification process. Therefore, harmonic excitations should be detected and isolated from the estimation of the structure's modal parameters.

Emerged in the audio domain for sources demixing from the audio records [2], the blind source separation (BSS) techniques have widely deployed in different research areas [3–8]. Castiglione *et al.* [9] recently proposed a solution to the BSS approach based on multi-filters designed in the frequency domain. The method's main idea is to divide a large underdetermined problem in the frequency axis into several overdetermined or determined problems in sub-bands. The modal parameters can then be estimated in the sub-bands. Thus, the method can handle the issue of severely underdetermined scenarios. In OMA, these techniques are used for finding latent sources from registered signals of systems without using any information about the mixing process. The state of the art in BSS for OMA has been comprehensively treated in [10].

The main challenge for applying the BSS techniques in OMA is when the number of measurement signals (or sensors) is less than that of latent sources—an underdetermined case. This problem can be encountered in many practical applications with limited measurements, for example, for complex structures or in the presence of harmonic excitations, when the measurement signals may be insufficient compared to the number of hidden sources.

There are some well-known indicators used in OMA to distinguish between the harmonic components and the structural components. Initially pointed out in study [11], kurtosis value has been widely used to distinguish between harmonic and modal responses [12–17]. If a component is pure harmonic, the graph of its probability density function (PDF) will have two peaks with the kurtosis value of 1.5. Otherwise, the PDF of a pure structural mode response will have a normal distribution with the kurtosis value equal to 3. Another effective tool to distinguish a structural component from a harmonic one is the modal assurance criterion (MAC) [18]. If a linear relationship exists between the two modal vectors, the MAC value will be near 1. If they are linearly independent, the MAC value will be near zero. In addition to the above-mentioned techniques, there is a direct approach for distinguishing harmonic components. This method proposes to consider them as zero-damping modes, while the damping ratio of the real pole of the structural component varies between 0.1% and 2% [12]. However, this method would not be effective when the structural modes have very low damping or the harmonic frequencies are very close to the structural frequencies [16].

The PARAFAC decomposition technique [19] was recently employed in operation modal analysis as one of the BSS family methods. It has been proven to effectively treat different types of excitations such as ambient vibrations, earthquakes, or human-induced vibrations [20–27]. It was showed that the method could handle a system with many modes, in which each mode has a different damping level [22, 27]. A simplified description of these methods can be summarized in three steps. At the first step, the covariance matrices of system responses are used to construct a third-order tensor. The PARAFAC technique is then used to decompose this third-order tensor into a sum of triple vectors' outer products. And finally, the obtained decomposition products like the mixing matrix and the auto-covariance matrix are used to estimate the system modal parameters.

Among the PARAFAC decomposition technique applications, Sadhu *et al.* [25] proposed a new approach based on a multiple-rank PARAFAC decomposition. In order to distinguish between sources corresponding to harmonic components or structural modes, the average kurtosis value is used. The authors proved that this approach is efficient for modal identification under the presence of multiple harmonic excitations.

However, the PARAFAC decomposition results in the auto-covariance functions of modal coordinates rather than direct modal coordinates. Because of the decaying feature of the auto-covariance functions of modal coordinates [28], the kurtosis values depend on the lengths of these functions. As a consequence, the insufficient length of the auto-covariance function can

cause inaccuracy when using kurtosis value as a harmonic indicator. Hence, for OMA, the length of the auto-covariance function needs to be considered when using kurtosis value as a harmonic indicator in PARAFAC decomposition-based methods.

To the best of our knowledge, there have been no studies on the influence of the length of the auto-covariance function on its kurtosis value.

This work takes advantage of previous studies. A modified procedure of the PARAFAC decomposition-based method is presented for the OMA. The minimum length of auto-covariance functions using natural periods and damping factors are suggested to distinguish between harmonic and modal components accurately. This modification allows to effectively distinguishing separated structural modes and harmonic ones. The efficiency in the performance of the proposed procedure has been verified using numerical and experimental tests. The rest of the paper is organized as follows. Section 2 describes the techniques of BSS and PARAFAC decomposition, Section 3 formulates a proposed procedure. The validation of the proposed procedure is presented in Section 4. Finally, Section 5 presents a conclusion.

2. Theoretical formulation

2.1. Instantaneous mixing model and PARAFAC decomposition

A linear instantaneous mixing model

$$\mathbf{x}(t) = \mathbf{A}\mathbf{s}(t) + \mathbf{n}(t) = \sum_i^{n_s} \mathbf{A}_i \mathbf{s}_i(t) + \mathbf{n}(t), \tag{1}$$

where $\mathbf{x}(t) = [x_1(t), x_2(t), \dots, x_{n_x}(t)]^T$ is n_x output measurements, $\mathbf{s}(t) = [s_1(t), s_2(t), \dots, s_{n_s}(t)]^T$ contains n_s latent sources, $\mathbf{n}(t)$ is the noisy vector, and \mathbf{A}_i is the i th column of the unknown mixing matrix \mathbf{A} . BSS aims to obtain the latent sources $\mathbf{s}(t)$ from the output measurement $\mathbf{x}(t)$ only. Depending on the relation between the number of measurement sensors and the number of sources, BSS problems can be classified as overdetermined case, when $n_x > n_s$, determined case, when $n_x = n_s$, or underdetermined case, when $n_x < n_s$.

Consider a classically damped system with n degrees of freedom subjected to excitation $\mathbf{f}(t)$ as follows:

$$\mathbf{M}\ddot{\mathbf{x}}(t) + \mathbf{C}\dot{\mathbf{x}}(t) + \mathbf{K}\mathbf{x}(t) = \mathbf{f}(t), \tag{2}$$

where $\mathbf{x}(t)$ is the vector of displacements; \mathbf{M} , \mathbf{C} , \mathbf{K} are mass, damping, and stiffness matrix, respectively.

The displacement $\mathbf{x}(t)$ can be represented in the form of a modal superposition of the vibration modes

$$\mathbf{x}(t) = \mathbf{\Phi}\mathbf{q}(t), \tag{3}$$

where $\mathbf{\Phi}$ is the mode shape matrix and $\mathbf{q}(t)$ is a column vector of modal coordinates.

Consider the similarity between (1) and (3), the modal coordinates $\mathbf{q}(t)$ and the mode shape matrix $\mathbf{\Phi}$ can be considered as the sources and the mixing matrix without the presence of noise, respectively.

The noise term $\mathbf{n}(t)$ in (1) is an additive noise assumed to be white. Therefore, its effect in the covariance function is zero at the time-lag τ_k different from zero. The covariance matrix $\mathbf{C}_x(\tau_k)$ of vibration measurements $\mathbf{x}(t)$ evaluated at time-lag τ_k can be written as follows:

$$\mathbf{C}_x(\tau_k) = E\{\mathbf{x}(t)\mathbf{x}^T(t + \tau_k)\} = \mathbf{\Phi}\mathbf{C}_q(\tau_k)\mathbf{\Phi}^T. \tag{4}$$

The auto-covariance matrix $\mathbf{C}_q(\tau_k)$ of modal coordinates (sources) at a time-lag τ_k is defined as

$$\mathbf{C}_q(\tau_k) = E\{\mathbf{q}(t)\mathbf{q}^T(t + \tau_k)\} \tag{5}$$

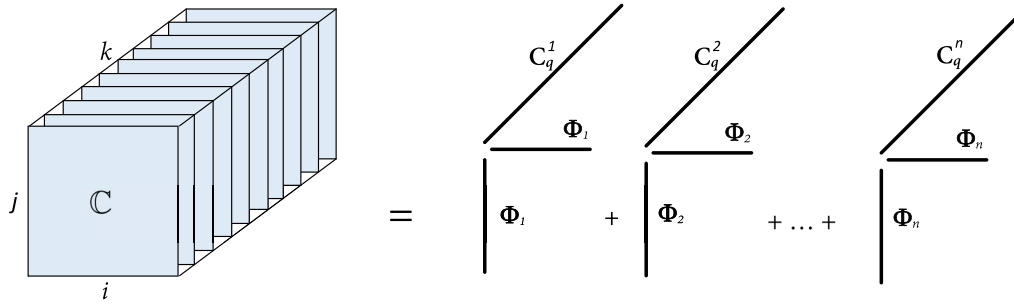


Figure 1. Geometric interpretation for PARAFAC decomposition [33].

and

$$C_{\mathbf{q}}^{ij}(\tau_k) = E\{q_i(t)q_j^T(t + \tau_k)\} = C_{\mathbf{q},k}^{ij} \tag{6}$$

The modal coordinates are considered to be mutually uncorrelated $C_{\mathbf{q},k}^{ij} = 0 \ \forall i \neq j$.

In the case of a 2-DOF system, $\mathbf{x}(t) = [x_1(t), x_2(t)]^T$. The covariance matrix of the responses at a time-lag τ_k is represented as follows:

$$\begin{bmatrix} C_{\mathbf{x},k}^{11} & C_{\mathbf{x},k}^{12} \\ C_{\mathbf{x},k}^{21} & C_{\mathbf{x},k}^{22} \end{bmatrix} = \begin{bmatrix} \phi_{11} & \phi_{12} \\ \phi_{21} & \phi_{22} \end{bmatrix} \begin{bmatrix} C_{\mathbf{q},k}^{11} & 0 \\ 0 & C_{\mathbf{q},k}^{22} \end{bmatrix} \begin{bmatrix} \phi_{11} & \phi_{21} \\ \phi_{12} & \phi_{22} \end{bmatrix}, \tag{7}$$

where

$$C_{\mathbf{x},k}^{ij} = \phi_{i1}\phi_{j1}C_{\mathbf{q},k}^{11} + \phi_{i2}\phi_{j2}C_{\mathbf{q},k}^{22} = \sum_{r=1}^2 \phi_{ir}\phi_{jr}C_{\mathbf{q},k}^{rr}. \tag{8}$$

For a general n -DOF system, the correlation between response signals at a time-lag τ_k can be represented by the following equation

$$C_{\mathbf{x},k}^{ij} = \sum_{r=1}^n \phi_{ir}\phi_{jr}C_{\mathbf{q},k}^{rr}. \tag{9}$$

Equation (9) can be treated by the joint approximate diagonalization technique employed in conventional second-order blind identification [4]. However, this method is only applicable to determined or overdetermined cases.

In order to deal with the underdetermined problem, Lathauwer and Castaing [29] introduced a simultaneous matrix diagonalization technique. A third-order tensor \mathbb{C} constructed from the covariance matrices $C_{\mathbf{x}}(\tau_k)$ can be treated by a PARAFAC decomposition [19]. This decomposition gives a mixing matrix and a matrix containing auto-covariance functions of modal coordinates.

The third-order tensor \mathbb{C} can be decomposed to n rank-one tensors as follows:

$$\mathbb{C} = \sum_{r=1}^n \Phi_r \circ \Phi_r \circ \mathbf{C}_{\mathbf{q}}^r \Leftrightarrow C_{\mathbf{x},k}^{ij} = \sum_{r=1}^n \phi_{ir}\phi_{jr}C_{\mathbf{q},k}^{rr}, \tag{10}$$

where \circ denotes the tensor outer product, and Φ_r and $\mathbf{C}_{\mathbf{q}}^r$ is the r th column of Φ and $\mathbf{C}_{\mathbf{q}}$, respectively.

As a consequence that tensor decomposition can be used to estimate mixing matrix Φ and auto-covariance functions of modal coordinates in matrix $\mathbf{C}_{\mathbf{q}}$. Several algorithms have been developed to fit a PARAFAC model, which can be classified into three categories: alternating algorithms, derivative-based algorithms, and non-iterative algorithms [30–32]. The geometric interpretation for the above equation can be represented as shown in Figure 1 [33].

Unlike singular value decomposition used for matrix cases, PARAFAC decomposition offers an additional advantage: it gives a unique decomposition even if its rank order is greater than the smallest dimension of the tensor. This property of PARAFAC decomposition can be utilized

Table 1. Number of identifiable sources with the number of measurements [34]

Number of measurements n_x	2	3	4	5	6	7	8	9	10
Number of identifiable sources n_{\max}	2	4	6	10	15	20	26	33	41

to deal with underdetermined cases in BSS. Stegeman *et al.* [34] derived the uniqueness for the decomposition if the inequality equation between the number of measurements n_x and the number of latent sources n_s is satisfied:

$$\frac{n_s(n_s - 1)}{2} \leq \frac{n_x(n_x - 1)}{4} \left(\frac{n_x(n_x - 1)}{2} + 1 \right) - \frac{n_x!}{(n_x - 4)!4!} (n_x)_{(n_x \geq 4)}, \tag{11}$$

where

$$\begin{aligned} (n_x)_{(n_x \geq 4)} &= 0 && \text{if } n_x < 4 \\ (n_x)_{(n_x \geq 4)} &= 1 && \text{if } n_x \geq 4. \end{aligned} \tag{12}$$

The relationship between the number of measurements and the maximal number of identifiable sources extracted using the PARAFAC decomposition is presented in Table 1.

2.2. PARAFAC decomposition for modal analysis

In BSS, the conventional kurtosis value can be used to distinguish modal responses and harmonic components. Besides, it has also been applied to a decay signal or the auto-covariance functions of modal responses [25, 35]. The kurtosis value of a zero-mean random variable x is defined as follows:

$$k = \frac{E\{x^4\}}{(E\{x^2\})^2}, \tag{13}$$

where E is the expectation operator.

For sampled data with K samples, the expectation can be computed statistically as follows:

$$E\{x\} = \frac{1}{K} \sum_{k=0}^K x(k). \tag{14}$$

The existing PARAFAC decomposition can deal with underdetermined cases, and it also works well with the presence of harmonic excitations. In the case of harmonic excitations, kurtosis values of separated auto-covariance functions can be used to distinguish between the harmonic components and structural modes.

The main steps for modal analysis of the PARAFAC decomposition-based method can be presented as follows [25]:

- Step 1: Collect responses $\mathbf{x}(t)$.
- Step 2: Build a third-order tensor \mathbb{C} from $\mathbf{C}_x(\tau_k)$ using (4).
- Step 3: Perform rank $R = 2 : n_{\max}$ PARAFAC decomposition of the tensor \mathbb{C} to obtain \mathbf{C}_q and mixing matrix \mathbf{A} . Estimate frequencies \mathbf{f} , damping ratios $\boldsymbol{\xi}$, and kurtosis values $\boldsymbol{\kappa}$ from \mathbf{C}_q .
- Step 4: Build a stability diagram and calculate the average kurtosis values \mathbf{k} at the estimated frequencies from the results in step 3.
- Step 5: Determine the number of active modes R_r , identify structural modes corresponding to the average kurtosis values $k \geq 3$, and harmonic components with $k < 3$ from the stability diagram.
- Step 6: Use the results of rank R_r PARAFAC decomposition and obtain modal parameters by eliminating harmonic components.

Table 2. Modal parameters of the numerical system are estimated with the proposed procedure under different kinds of excitations

Mode		1	2	3	4
Exact	f (Hz)	1.24	3.59	6.81	
	ξ (%)	1.31	0.50	0.34	
Initial displacement	f (Hz)	1.24	3.59	6.81	
	ξ (%)	1.29	0.51	0.38	
	Kurtosis	3.9	3.9	3.9	
Random noise	Nature	Struct	Struct	Struct	
	f (Hz)	1.24	3.59	6.81	
	ξ (%)	1.42	0.46	0.38	
	Kurtosis	4.0	3.9	4.0	
Presence of harmonics	Nature	Struct	Struct	Struct	
	f (Hz)	1.24	3.59	6.81	10.00
	ξ (%)	1.42	0.46	0.39	0.00
	Kurtosis	4.0	3.9	4.1	1.5
	Nature	Struct	Struct	Struct	<i>Harmonic</i>

The kurtosis values are estimated with $T_L^i = (40T_i)/(\xi_i)$.

In the method, the modal parameters can be extracted from the auto-covariance functions using the logarithmic decrement method in the time domain or the single-mode curve fitting method in the frequency domain.

2.3. Illustration

Consider an example of a 3-DOF mass–spring–damper system with the mass matrix \mathbf{M} and the stiffness matrix \mathbf{K} :

$$\mathbf{M} = \begin{bmatrix} 2 & 0 & 0 \\ 0 & 2 & 0 \\ 0 & 0 & 2 \end{bmatrix}; \quad \mathbf{K} = \begin{bmatrix} 200 & -360 & 120 \\ -360 & 2000 & -1300 \\ 120 & -1300 & 2600 \end{bmatrix}.$$

The damping matrix \mathbf{C} is calculated through a proportional damping model $\mathbf{C} = 0.2\mathbf{M} + 0.00005\mathbf{K}$. The three exact natural frequencies and the three damping ratios are presented in Table 2.

The exact mode shape matrix is as follows:

$$\Phi = \begin{bmatrix} 1.0000 & 1.0000 & 1.0000 \\ 0.2480 & -3.1550 & -6.8089 \\ 0.0816 & -2.6650 & 8.4359 \end{bmatrix}.$$

The system is subjected to an initial displacement $x_3(0) = 1$ with zero velocity. Responses are simulated for a duration of 50 s with a sampling rate of 200 Hz. The responses of 3 DOFs of the system are presented in Figure 2a. For the illustration, the covariance matrix is calculated with the total of 3000 time-lag points (15 s).

Following the steps of the existing PARAFAC decomposition-based method, a stability diagram is built with different rank R PARAFAC decomposition values ranging from 2 to 4 (corresponding to three signals).

Three average kurtosis values corresponding to three active modes in the diagram are shown in Figure 2b. The first two kurtosis values are less than 3. This means that these two first frequencies belong to harmonic excitation, according to step 5. This is an incorrect result since

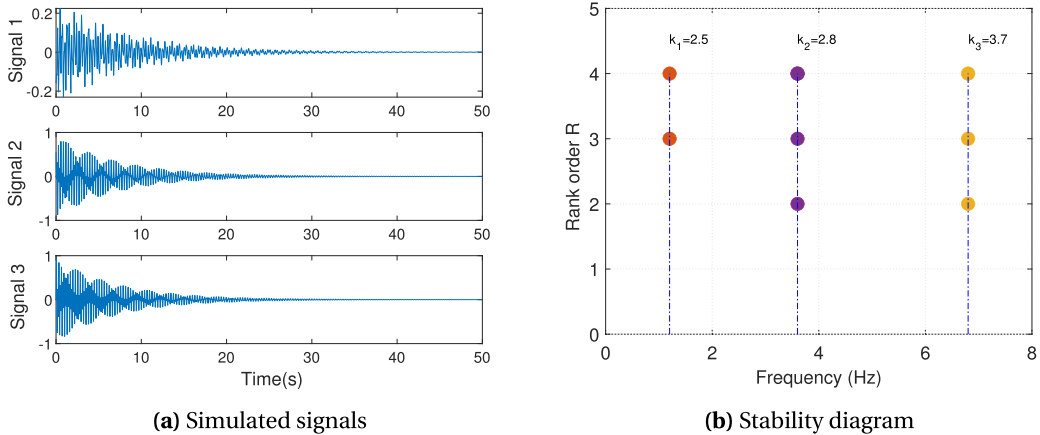


Figure 2. Responses (left) and stability diagram obtained from the PARAFAC decomposition-based method (right).

these active modes are the structural modes in this example. This is due to the lengths of auto-covariance functions used for calculating kurtosis values are not sufficient. The existing PARAFAC decomposition-based method does not give a rule for choosing the length of the auto-covariance of the modal coordinates. To overcome this limitation and improve the existing method, the presented study proposes to select the length of the auto-covariance function while using the kurtosis value as a harmonic indicator.

3. Enhanced procedure for the PARAFAC decomposition-based method

The previous illustration shows that it is necessary to have an adequate length of auto-covariance function for accurate modal identification and an efficient distinction of structural modes and harmonic components. Since the decaying feature of the auto-covariance function [28] this decaying feature causes a variation of the auto-covariance function’s statistical characteristic when the length of the auto-covariance function changes. Therefore, using kurtosis value as a harmonic indicator to distinguish between harmonic components and modal ones needs to consider the length of auto-covariance functions in PARAFAC decomposition-based methods in the OMA.

Kurtosis is well-known as a measure of the “tailedness” of the probability distribution that differs from the tails of a normal distribution. The modal coordinate has a normal distribution, and its kurtosis value equals 3. However, the decaying nature of the auto-covariance function makes the graph of its distribution being more narrow near the peak when the length of the auto-covariance functions is longer. It means that an auto-covariance function’s kurtosis value becomes more than 3 if its length is longer than a certain value. The auto-covariance function of a harmonic component has a different feature than that of the modal coordinate’s auto-covariance function. The kurtosis value of the auto-covariance function of a harmonic component is about 1.5 regardless of the length of its auto-covariance function.

3.1. The effect of signal length on kurtosis value

Under free vibration, the modal coordinate is the response of a single degree of freedom system that has a form as follow:

$$q_i(t) = A_i e^{-2\xi\pi f_{ni}t} \sin(2\pi f_{di}t + \theta_i), \tag{15}$$

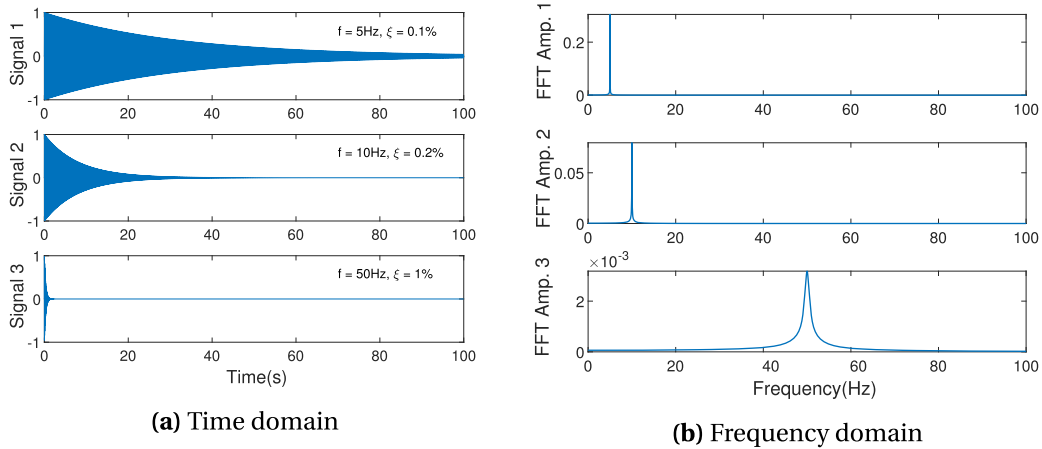


Figure 3. Three decaying signals.

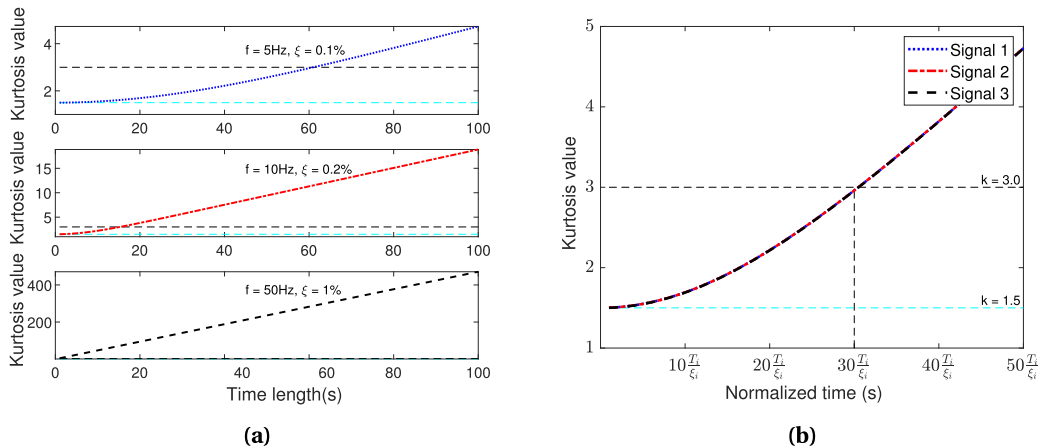


Figure 4. Kurtosis with length variation of the decaying signals.

where f_{ni} , ξ_i , θ_i , and A_i are the natural frequency, the damping ratio, the phase, and the amplitude of the i th mode, respectively.

It was proven that the auto-covariance functions of responses have a decaying form [36] that is similar to those in (15). Thus, the auto-covariance functions can be treated as free vibration signals [37].

Decaying vibration signals with different natural frequencies and damping ratios are used to illustrate the influence of their length on kurtosis value. These signals last for 100 s, as seen in Figure 3.

It takes about 60 s for the kurtosis value to become equal to 3 for the first signal in Figure 4a. Less than this duration, its kurtosis values will be smaller than 3. However, less time is needed for the second and the third ones to their kurtosis values higher than 3.

Because of the decaying feature of these signals, not only the kurtosis value depends on the natural period, but it also depends on the signal's damping ratio. The kurtosis value of the auto-covariance function increases in the function of the period T_i and increases inversely in the damping ratio ξ_i function.

Therefore, this study considers the simultaneous influence of frequency and the damping coefficient on the kurtosis values. Figure 4b draws kurtosis values in a function of t_i with t_i defined in (16)

$$t_i = \frac{T_i}{\xi_i}, \tag{16}$$

where ξ is in percentage value, T_i is in second.

According to the numerical simulations that were carried out, one can conclude that the kurtosis reaches a value of 3 after approximately $30t_i$. Figure 4b shows that the kurtosis value reaches 3 in about $30t_i$ for the given example. Consequently, the auto-covariance functions' length should be at least $30t_i$, as presented in (17)

$$T_L^i > 30t_i = \frac{30T_i}{\xi_i}. \tag{17}$$

In the case of an auto-covariance function with a damping ratio identified smaller than 0.1%, the length of auto-covariance functions is selected by (18)

$$T_L^i > 30t_i = \frac{30T_i}{0.1}. \tag{18}$$

In this study, kurtosis values estimated with a time length $T_L^i = 40t_i$ is used for distinguishing between harmonic components and structural modes.

3.2. The improvement procedure

The above choice of the time length of the auto-covariance functions is integrated into the proposed procedure.

Here are the proposed steps for the PARAFAC decomposition-based method in OMA.

- Step 1: Collect responses $\mathbf{x}(t)$.
- Step 2: Build a third-order tensor \mathbb{C} from $\mathbf{C}_x(\tau_k)$.
- Step 3: Perform rank $R = 2 : n_{\max}$ PARAFAC decomposition of the tensor \mathbb{C} to obtain \mathbf{C}_q and mixing matrix \mathbf{A} . Estimate frequencies \mathbf{f} from \mathbf{C}_q .
- Step 4: Build a stability diagram and determine the number of active modes R_r .
- Step 5: Use the result of rank R_r PARAFAC decomposition. Recognize harmonic components with kurtosis value $k \approx 1.5$, or structural modes with $k \geq 3.0$ based on a choice of the time length of auto-covariance functions as follows:

$$\begin{cases} T_L^i > \frac{30T_i}{\xi_i} & \text{if } \xi_i \geq 0.1(\%) \\ T_L^i > \frac{30T_i}{0.1} & \text{if } \xi_i < 0.1(\%). \end{cases} \tag{19}$$

- Step 6: Obtain modal parameters by eliminating harmonic components.

4. Application

To validate the effectiveness of the proposed procedure, numerical and experimental tests were carried out for various excitation cases.

4.1. Numerical simulations

The numerical model used in Section 2.3 will be reutilized in this part. Modal identifications are performed for different cases like initial displacement, white noise excitation, and white noise accompanied by a harmonic excitation.

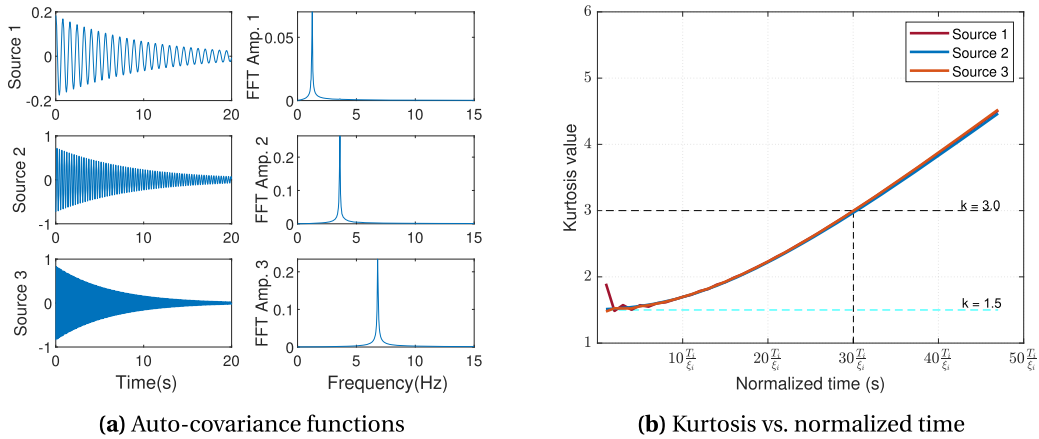


Figure 5. Auto-covariance functions and kurtosis in the case of an initial displacement.

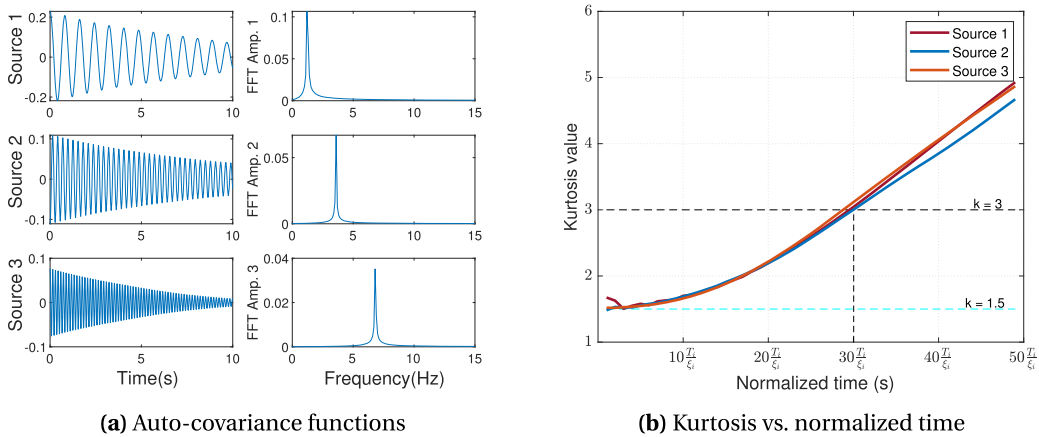


Figure 6. Auto-covariance functions and kurtosis values in the case of random noise.

4.1.1. *The numerical system subjected to an initial displacement*

The proposed procedure was applied to the simulated responses used in Section 2.3. Three auto-covariance functions corresponding to rank $R = 3$ PARAFAC decomposition are shown in Figure 5a.

To illustrate the proposed procedure’s effectiveness, the curves of kurtosis values corresponding to different lengths of the auto-covariance functions are presented in Figure 5b. One can realize that auto-covariance functions’ lengths should be longer than $30 \times (T_i) / (\xi_i)$ to make kurtosis values higher than 3, as seen in Figure 5b. The identified modal parameters are the same as the exact ones, as seen in Table 2.

4.1.2. *The numerical system subjected to random noise excitation*

In this numerical test, random excitations were applied at all three DOFs of the system. The responses in the displacements of three DOFs were obtained by integrating the motion equation with the Runge–Kutta algorithm. The sampling rate was 200 Hz for a duration of 600 s.

The proposed procedure was then applied to this case. Three auto-covariance functions corresponding to rank $R = 3$ PARAFAC decomposition are shown in Figure 6a. The curves of

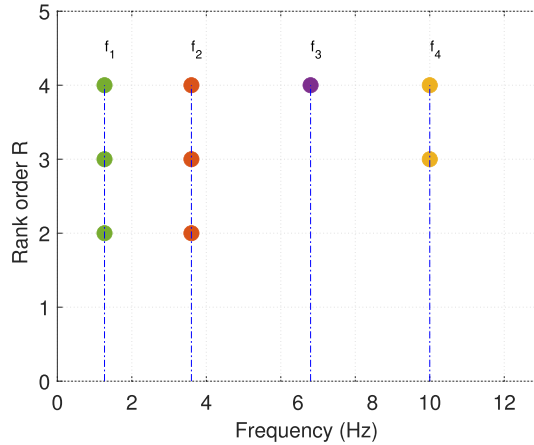


Figure 7. Stability diagram in the case of random noise accompanied by harmonic excitation.

kurtosis values corresponding to their different lengths are presented in Figure 6b. One can realize that auto-covariance functions' lengths should be longer than $30 \times (T_i)/(\xi_i)$ to make kurtosis higher than 3, as seen in Figure 6b. The identified modal parameters are close to the exact ones, as shown in Table 2.

4.1.3. *The numerical system subjected to random noise accompanied by a harmonic excitation*

In this numerical test, random excitations accompanied by a harmonic excitation were applied at all three DOFs of the system. The displacement of three DOFs was obtained by integrating the motion equation with the Runge–Kutta algorithm. The sampling rate was 200 Hz for a duration of 600 s.

The proposed procedure is now implemented to identify the modal parameters of the system. A stability diagram is built from different values of rank R PARAFAC decompositions, as seen in Figure 7. One can see that there are four active modes in this case.

The auto-covariance functions corresponding to rank $R = 4$ PARAFAC decomposition are shown in Figure 8a. The curves of kurtosis values corresponding to their different lengths are presented in Figure 8b. The figure shows that the first three components' kurtosis values (corresponding to source 1, source 2, and source 3) are higher than 3.0 when lengths of auto-covariance functions are longer than $30 \times (T_i)/(\xi_i)$. It means that these components belong to the structural modes. The last component (corresponding to source 4) with a kurtosis value of 1.5 corresponds to harmonic excitation. The MAC diagram shows a good correlation, as presented in Figure 9. The modal parameters are presented in Table 2, and they are close to the exact ones.

4.2. *Experimental tests*

To validate the proposed procedure's efficiency, a series of experimental tests were carried out, as shown in Figure 10. The tests were conducted for a steel cantilever beam with Young's modulus $E = 200,000$ MPa, and density $\rho = 7850$ kg/m³. The cantilever beam of 0.8 m in length, 0.04 m in width, and 0.006 m in height were used for experimental tests under different excitation patterns. The responses of the cantilever beam were recorded at a sampling rate of 2048 Hz.

Initially, an analytical computation of the first five natural frequencies of the considered beam was performed. Its analytical frequencies are given in Table 3. To obtain a reference

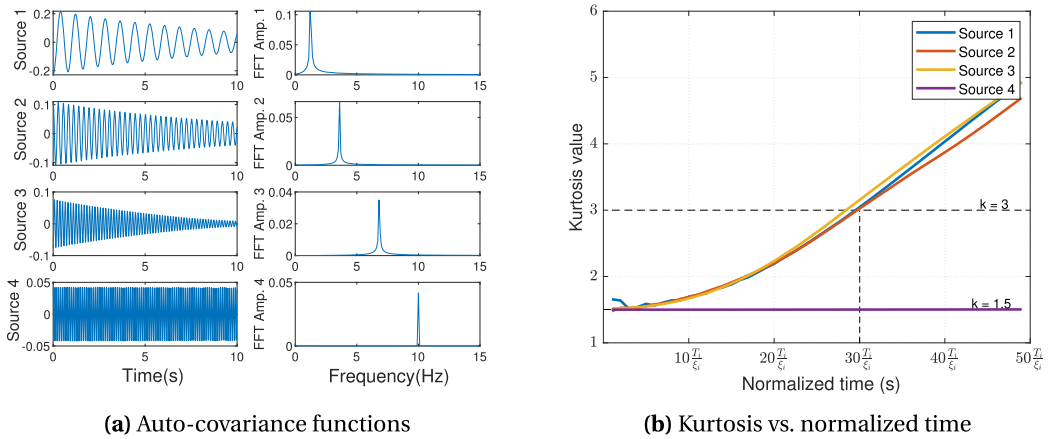
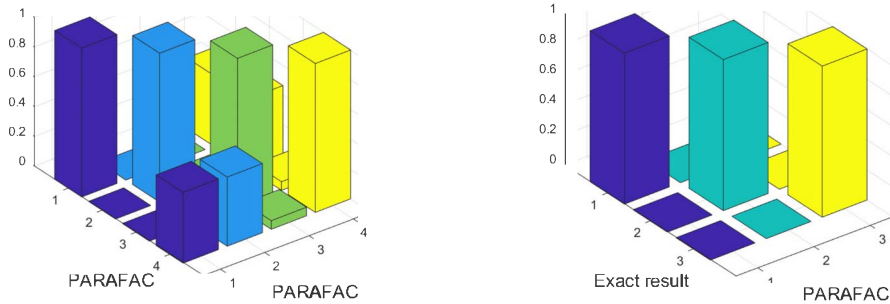


Figure 8. Auto-covariance functions and kurtosis values in the case of random noise accompanied by harmonic excitation.



(a) Auto MAC before harmonic component removal **(b)** Cross MAC after harmonic component removal

Figure 9. Mode shape comparison in the case of random noise accompanied by harmonic excitation.

Table 3. Modal parameters of the cantilever beam are estimated by the proposed procedure under different kinds of excitations, and kurtosis values are estimated with $T_L^i = (40T_i)/(\xi_i)$

Mode		1	2	3	4	5	6
Analytical	f (Hz)	7.64	47.90	134.14	262.85	433.52	
	ξ (%)	1.23	0.28	0.45	0.66	0.17	
B&K software	f (Hz)	7.28	46.82	131.43	260.86	427.86	
	ξ (%)	1.38	0.35	0.52	0.63	0.12	
	Kurtosis	3.8	3.9	3.8	3.9	4.0	
Gaussian noise	f (Hz)	7.32	46.73	131.23	260.44	428.00	
	ξ (%)	1.38	0.35	0.52	0.63	0.12	
	Kurtosis	3.8	3.9	3.8	3.9	4.0	
Presence of harmonics	f (Hz)	7.28	19.99	46.54	130.60	259.88	427.81
	ξ (%)	1.11	0.00	0.32	0.52	0.63	0.13
	Kurtosis	3.8	1.5	3.9	3.8	3.8	3.8
	Nature	Struct	<i>Harmonic</i>	Struct	Struct	Struct	Struct

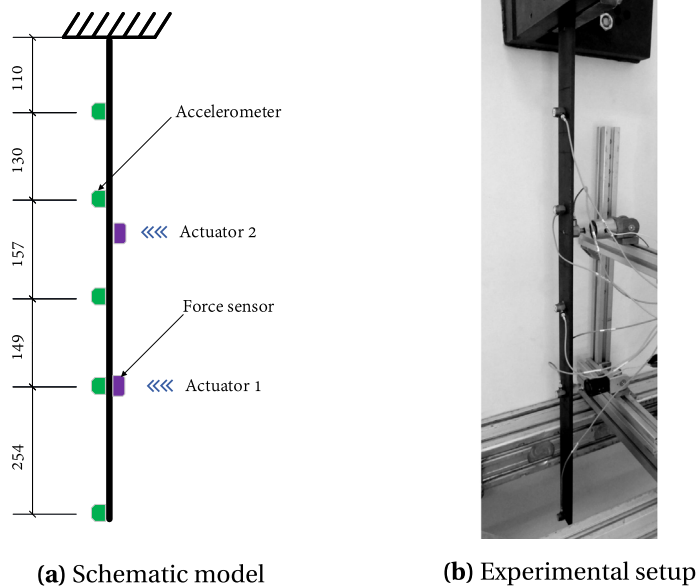


Figure 10. The cantilever beam and test point locations.

model, a classical experimental modal analysis was performed using a shaker at a location on the cantilever beam. The time responses were recorded using five B&K Type 4533-B-001 accelerometers mounted along the length of the cantilever beam. A B&K Type 8230-001 force transducer is also used to collect the input excitation, as shown in Figure 10. The commercial B&K Connect™ software acquires signals from the force sensor and the accelerators for input-output modal identification. The results of modal parameter identification are given in Table 3.

Two following experimental examples are considered to demonstrate the efficiency of the proposed procedure on actual measurements. The first example represents a determined case when the measurements equal the number of the structural modes. The second example illustrates an underdetermined problem where five sensors are used to separate six components: five structural modes and a harmonic component.

4.2.1. *The structure subjected to Gaussian noise excitation*

In this experiment, an actuator was used to create a band-limited Gaussian noise excitation with a 0–500 Hz pass-band.

The proposed procedure was then applied to the measurement data. A stability diagram is built with different rank R PARAFAC decomposition values ranging from 2 to 10 (corresponding to five measurement signals). The diagram shows that there are five active modes, as seen in Figure 11.

Five auto-covariance functions corresponding to rank $R = 5$ PARAFAC decomposition are shown in Figure 12a. The curves of kurtosis values estimated with different lengths of the auto-covariance functions are presented in Figure 12b. All kurtosis values of the auto-covariance functions are higher than 3.0 when their lengths are longer than $30 \times (T_i)/(\xi_i)$. Hence, it means that these active modes belong to the cantilever beam.

These results are compared to those identified by the software, as shown in Table 3. These estimated modal parameters match well with those identified by the software. The MAC shows

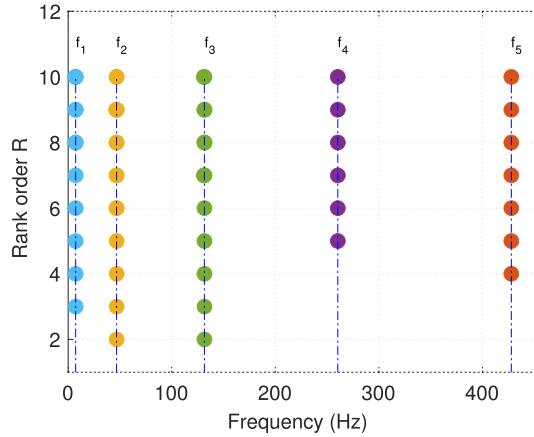


Figure 11. Stability diagram in the case of Gaussian noise excitation.

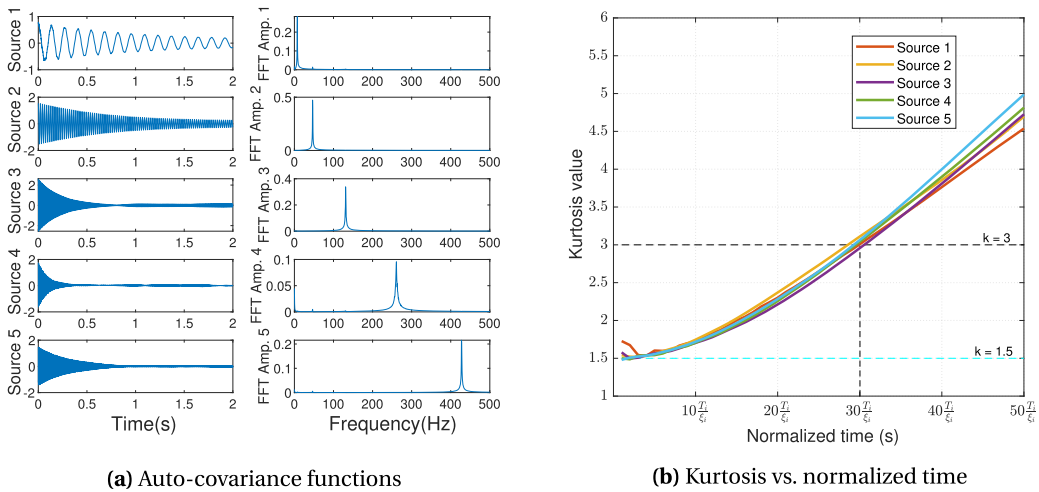


Figure 12. Auto-covariance functions and kurtosis values in the case of Gaussian noise excitation.

a good correlation between the structural mode shapes obtained by two different methods with the auto-correlation coefficients approximate 1, as seen in Figure 13.

4.2.2. *The structure subjected to Gaussian noise accompanied by a harmonic excitation*

In this experiment, in addition to a band-limited Gaussian noise excitation with a pass-band of 0 to 500 Hz, the cantilever beam was also subjected to a harmonic excitation at 20 Hz.

The proposed procedure was then applied to the measurement data. A stability diagram is built with different values of rank R PARAFAC decomposition ranging from 2 to 10. There are six active modes, as found in Figure 14. These six auto-covariance functions corresponding to rank $R = 6$ PARAFAC decomposition are shown in Figure 15a.

The curves of kurtosis values estimated with different lengths of the auto-covariance functions are presented in Figure 15b. The second separated component belongs to the harmonic excitation because this component's kurtosis values remain the same with the different lengths of its auto-covariance function. Its kurtosis value is approximately 1.5 at the time length of

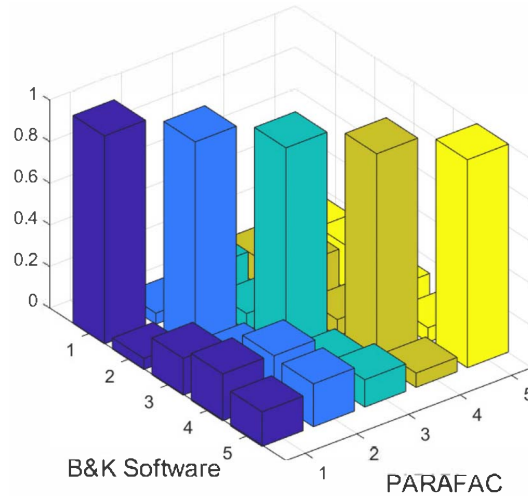


Figure 13. Mode shape comparison in the case of Gaussian noise excitation.

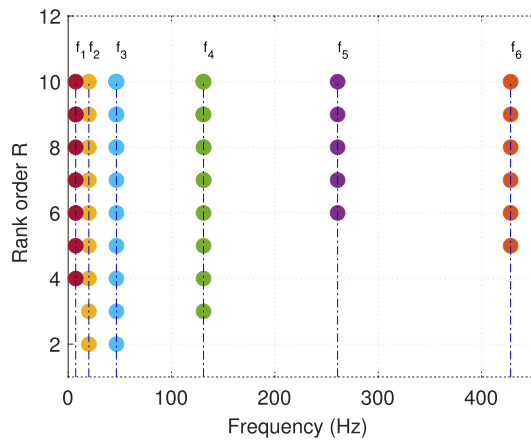


Figure 14. Stability diagram in the case of Gaussian noise accompanied by harmonic excitation.

$T_L^i = 40 \times (T_2)/(\xi_2)$. Other kurtosis values of the remaining auto-covariance functions are about 3.0 when their lengths are longer than a duration $T_L^i = 30 \times (T_i)/(\xi_i)$. The kurtosis values of these components with $T_L^i = 40 \times (T_i)/(\xi_i)$ are about 3.8, as given in Table 3. It means that these remaining active modes belong to the cantilever beam. The identified results are presented in Table 3. The MAC comparison is presented in Figure 16. It shows a good correlation.

5. Conclusions

The discussed method based on the PARAFAC decomposition has proven to be an effective tool for modal analysis in underdetermined cases. This method can also distinguish harmonic components and structural modes using kurtosis values estimated from the auto-covariance functions of modal coordinates. However, there was no explicit proposition for the choice of the length of the auto-covariance function, which led to an erroneous result when this length was insufficient.

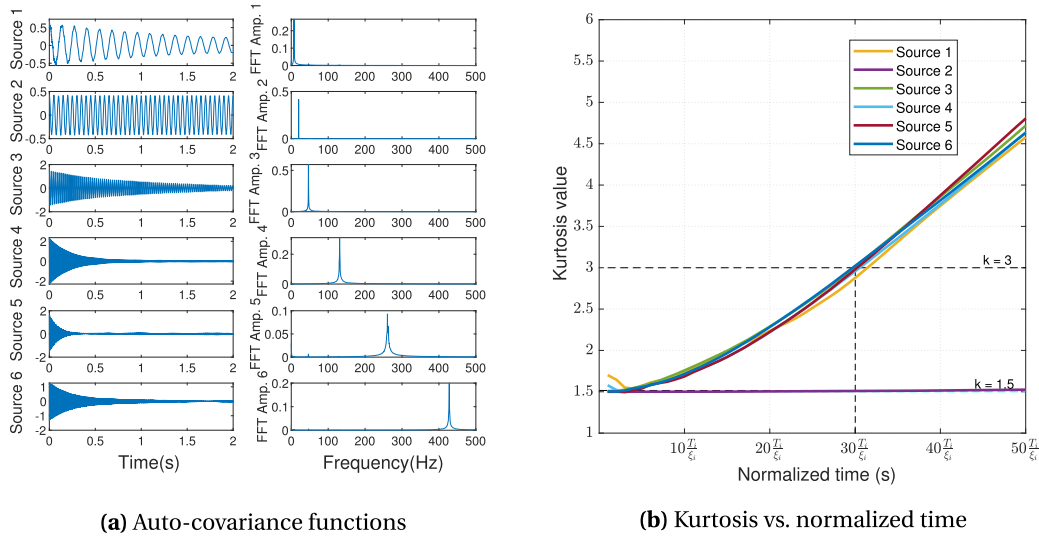
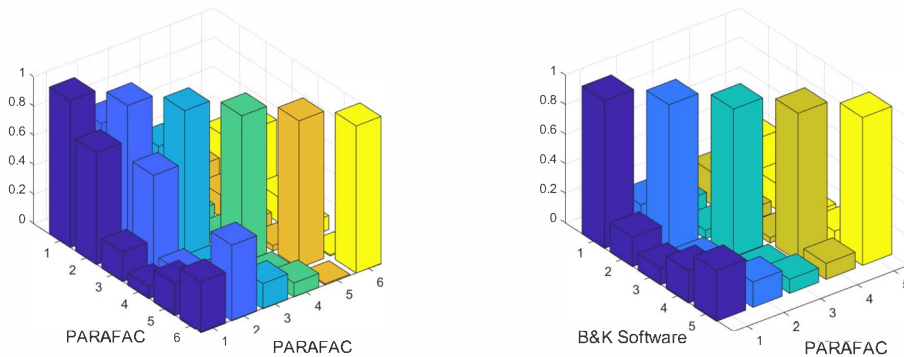


Figure 15. Auto-covariance functions and kurtosis values in the case of Gaussian noise accompanied by harmonic excitation.



(a) Auto MAC before harmonic component removal **(b)** Cross MAC after harmonic component removal

Figure 16. Mode shape comparison in the case of Gaussian noise accompanied by harmonic excitation.

This study illustrates the dependence of the kurtosis values on the lengths of the auto-covariance functions. The presented work allows one to make a conclusion about this length based on the modal period T_i and the damping ratio ξ_i . It turned out that for the correct separation of structural modes and harmonic components, the length of these auto-covariance functions must be greater than $30T_i/\xi_i$.

The proposed procedure was applied to numerical examples and then confirmed by experimental tests. To estimate the kurtosis values, the length of the auto-covariance function was fixed at $40T_i/\xi_i (> (30T_i)/(\xi_i))$.

For the numerical simulation part, the responses from the 3-DOF system under (i) random excitation and (ii) random excitation accompanied by harmonic excitation were processed in accordance with the proposed procedure. The revealed modal parameters are very close to the exact ones when the calculated values of kurtosis for the structural modes is ($k = 3.9-4.1$) and for the harmonic component is $k \approx 1.5$.

In the experimental test section, the proposed procedure is applied to the responses of the cantilever beam under (i) random excitation and (ii) random excitation mixed with harmonic excitation. The identified modal parameters by the proposed method are in good agreement with the reference ones obtained using the B&K software. In the presence of harmonic excitation, the calculated kurtosis values for the structural modes are close to 4.0, and for the harmonic component is approximate 1.5.

These validation tests confirm the effectiveness of the proposed method for use in OMA for underdetermined cases in general and cases with the presence of harmonic excitations, in particular.

Acknowledgment

The first author gratefully acknowledges the French Government's funding through the scholarship to undertake this work.

References

- [1] L. Zhang, R. Brincker, P. Andersen, "An overview of operational modal analysis: major development and issues", in *Proceedings of the 1st International Operational Modal Analysis* (Copenhagen), Aalborg Universitet, 2005.
- [2] J.-F. Cardoso, "Blind signal separation: statistical principles", *Proc. IEEE* **86** (1998), p. 2009-2025.
- [3] P. Comon, "Independent component analysis, a new concept?", *Signal Process.* **36** (1994), no. 3, p. 287-314.
- [4] A. Belouchrani, K. Abed-Meraim, J.-F. Cardoso, E. Moulines, "A blind source separation technique using second-order statistics", *IEEE Trans. Signal Process.* **45** (1997), p. 434-444.
- [5] A. Hyvärinen, E. Oja, "Independent component analysis: algorithms and applications", *Neural Netw.* **13** (2000), no. 4, p. 411-430.
- [6] P. P. Pokharel, U. Ozertem, D. Erdogmus, J. C. Principe, "Recursive complex BSS via generalized eigendecomposition and application in image rejection for BPSK", *Signal Process.* **88** (2008), no. 6, p. 1368-1381.
- [7] S. Xie, L. Yang, J.-M. Yang, G. Zhou, Y. Xiang, "Time-frequency approach to underdetermined blind source separation", *IEEE Trans. Neural Netw. Learn. Syst.* **23** (2012), no. 2, p. 306-316.
- [8] P. Bofill, M. Zibulevsky, "Underdetermined blind source separation using sparse representations", *Signal Process.* **81** (2001), no. 11, p. 2353-2362.
- [9] R. Castiglione, J. Antoni, L. Garibaldi, "Separation and identification of structural modes in largely underdetermined scenarios using frequency banding", *J. Sound Vib.* **414** (2018), p. 192-217.
- [10] A. Sadhu, S. Narasimhan, J. Antoni, "A review of output-only structural mode identification literature employing blind source separation methods", *Mech. Syst. Signal Process.* **94** (2017), p. 415-431.
- [11] T. Lago, "The difference between harmonics and stochastic narrow band responses", in *Presentation at the SVIBS Symposium* (Stockholm), Structural Vibration Solution, 1997.
- [12] V. Gagnol, T.-P. Le, P. Ray, "Modal identification of spindle-tool unit in high-speed machining", *Mech. Syst. Signal Process.* **25** (2011), p. 2388-2398.
- [13] N.-J. Jacobsen, P. Andersen, R. Brincker, "Eliminating the influence of harmonic components in operational modal analysis", in *The International Modal Analysis Conference IMAC-XXIV* (Orlando, USA), Society for Experimental Mechanics, 2007.
- [14] J. Antoni, "The spectral kurtosis: a useful tool for characterising non-stationary signals", *Mech. Syst. Signal Process.* **20** (2006), p. 282-307.
- [15] J. Antoni, "Blind separation of vibration components: Principles and demonstrations", *Mech. Syst. Signal Process.* **19** (2005), p. 1166-1180.
- [16] C. Rainieri, G. Fabbrocino, G. Manfredi, M. Dolce, "Robust output-only modal identification and monitoring of buildings in the presence of dynamic interactions for rapid post-earthquake emergency management", *Eng. Struct.* **34** (2012), p. 436-446.
- [17] R. Brincker, P. Andersen, N. B. Møller, "An indicator for separation of structural and harmonic modes in output-only modal testing", in *Proceedings of SPIE—The International Society for Optical Engineering* (Madrid, Spain), vol. 2, Aalborg University, 2000.
- [18] R. Allemang, "The modal assurance criterion—twenty years of use and abuse", *Sound Vib.* **37** (2003), p. 14-21.
- [19] R. A. Harshman, *Foundations of the PARAFAC Procedure: Models and Conditions for an Explanatory Multi-modal Factor Analysis*, University of California, Los Angeles, 1970.

- [20] J. Antoni, S. Chauhan, "An alternating least squares (ALS) based blind source separation algorithm for operational modal analysis", in *Proceedings of the 29th IMAC, A Conference and Exposition on Structural Dynamics* (New York, USA), Conference Proceedings of the Society for Experimental Mechanics Series, vol. 3, Springer, 2011, https://doi.org/10.1007/978-1-4419-9299-4_15.
- [21] S. I. McNeill, "Extending blind modal identification to the underdetermined case for ambient vibration", in *ASME 2012 International Mechanical Engineering Congress and Exposition* (Texas, USA), The American Society of Mechanical Engineers, 2012, <https://doi.org/10.1115/IMECE2012-93140>.
- [22] F. Abazarsa, S. F. Ghahari, F. Nateghi, E. Taciroglu, "Response-only modal identification of structures using limited sensors", *Struct. Control Health Monit.* **20** (2013), p. 987-1006.
- [23] F. Abazarsa, F. Nateghi, S. F. Ghahari, E. Taciroglu, "Blind modal identification of non-classically damped systems from free or ambient vibration records", *Earthq. Spectra* **29** (2013), p. 1137-1157.
- [24] F. Abazarsa, F. Nateghi, S. F. Ghahari, E. Taciroglu, "Extended blind modal identification technique for nonstationary excitations and its verification and validation", *J. Eng. Mech.* **142** (2015), p. 1-19.
- [25] A. Sadhu, A. Goldack, S. Narasimhan, "Ambient modal identification using multi-rank parallel factor decomposition", *Struct. Control Health Monit.* **22** (2015), p. 595-614.
- [26] A. Sadhu, B. Hazra, S. Narasimhan, "Decentralized modal identification of structures using parallel factor decomposition and sparse blind source separation", *Mech. Syst. Signal Process.* **41** (2013), p. 396-419.
- [27] P. Friesen, A. Sadhu, "Performance of tensor decomposition-based modal identification under nonstationary vibration", *Smart Mater. Struct.* **26** (2017), p. 1-19.
- [28] D. E. Newland, *An Introduction to Random Vibrations and Spectral Analysis*, Longman Group Limited, London, 1975.
- [29] L. D. Lathauwer, J. Castaing, "Blind identification of underdetermined mixtures by simultaneous matrix diagonalization", *IEEE Trans. Signal Process.* **56** (2008), p. 1096-1105.
- [30] G. Tomasi, R. Bro, "A comparison of algorithms for fitting the PARAFAC model", *Comput. Statist. Data Anal.* **50** (2006), no. 7, p. 1700-1734.
- [31] P. Comon, X. Luciani, A. de Almeida, "Tensor decompositions, alternating least squares and other tales", *J. Chemom.* **23** (2009), p. 393-405.
- [32] L. Lathauwer, D. Nion, "Decompositions of a higher-order tensor in block terms—Part III: alternating least squares algorithms", *SIAM J. Matrix Anal. Appl.* **30** (2008), p. 1067-1083.
- [33] A. Smilde, R. Bro, P. Geladi, *Multi Way Analysis—Applications in Chemical Sciences*, John Wiley Sons, Ltd, England, 2004.
- [34] A. Stegeman, J. M. F. T. Berge, L. D. Lathauwer, "Sufficient conditions for uniqueness in Candecomp/Parafac and Indscal with random component matrices", *Struct. Control Health Monit.* **71** (2006), p. 219-229.
- [35] S. McNeill, D. Zimmerman, "Relating independent components to free-vibration modal responses", *Shock Vib.* **17** (2010), p. 161-170.
- [36] G. James, T. Carne, J. Laufer, "The natural excitation technique (NExT) for modal parameter extraction from operating structures", *J. Anal. Exp. Modal Anal.* **10** (1995), p. 260-277.
- [37] B. Hazra, A. Roffel, S. Narasimhan, M. Pandey, "Modified cross-correlation method for the blind identification of structures", *J. Eng. Mech.* **136** (2010), p. 889-897.